

# OBSERVATIONS OF SPECTRAL AND TIME VARIABILITIES FROM MCG-2-58-22

CHUL-SUNG CHOI

Korea Astronomy Observatory, 36-1 Hwaam, Yusong, Taejon 305-348, Korea;  
cschoi@hanul.issa.re.kr

TADAYASU DOTANI

Institute of Space and Astronautical Science, 3-1-1 Yoshinodai, Sagamihara, Kanagawa  
229-8510, Japan; dotani@astro.isas.ac.jp

INSU YI

School of Physics, Korea Institute for Advanced Study, 207-43 Cheongryangri,  
Dongdaemun, Seoul 130-012, Korea; iyi@kias.re.kr

CHULHEE KIM

Department of Earth Science Education, Chonbuk National University, Chonju 516-756,  
Korea; chkim@astro.chonbuk.ac.kr

Received \_\_\_\_\_; accepted \_\_\_\_\_

## ABSTRACT

We present results from analysis of the X-ray archive data of MCG–2-58-22, acquired with ROSAT from 1991 to 1993 and with ASCA from 1993 to 1997. By analyzing light curves, we find that MCG–2-58-22 shows a clear time variability in X-ray flux. The time scales of the variations range widely from  $\sim 10^3$  s to more than years. Among the variations, a flare-like event overlaid on the gradual flux decrease from 1979 to 1993 is detected in the 1991 data; the flux has increased at least by a factor of 3. Combined analysis of the ROSAT and ASCA spectra shows that a simple absorbed power-law does not fit the overall energy spectra, unless the column density lower than the Galactic value ( $3.5 \times 10^{20} \text{ cm}^{-2}$ ) is adopted. We find the clear time variability of the spectra in the energy range of 0.1–2.0 keV. The spectral shape with respect to an adopted model continuum is generally correlated with their flux level. However, the flux variation does not result in any significant influences on their spectra in the energy range of 2–10 keV. As reported previously, there is an iron line centered at  $\sim 6.3$  keV (which is not corrected for the red-shift effect), but we find that the line width is broad  $\sigma = 0.9_{-0.3}^{+0.6}$  keV with a single Gaussian model. The implications of these observational results are discussed in terms of a supermassive black hole model and accretion flow dynamics near the central black hole.

*Subject headings:* galaxies:individual(MCG–2-58-22) — galaxies:nuclei — galaxies:Seyfert — X-rays:galaxies

## 1. INTRODUCTION

MCG–2-58-22 (Mrk 926) is an active galactic nucleus (AGN) optically classified as Seyfert 1 or 1.2 galaxy (Whittle 1992; Kotilainen & Martin 1994). It is located at a distance of 284 Mpc ( $z = 0.04732$  and  $H_0 = 50 \text{ km s}^{-1} \text{ Mpc}^{-1}$ ; Huchra et al. 1993). In X-ray band, the source has been observed frequently for more than two decades from the Einstein observatory to ASCA. Many observational results, however, still remain either to be understood or to be confirmed. Among those, the first is the “soft X-ray excess” problem, which in general is defined as emission that exceeds the extrapolation from the observed hard X-ray power-law continuum. Some authors have argued that they found an excess emission below 1–2 keV in their spectra of MCG–2-58-22 (e.g., Turner et al. 1991; Ghosh & Soundararajaperumal 1992; Piro, Matt, & Ricci 1997), but different authors have disagreed (Mushotzky 1984; Turner & Pounds 1989; Turner, George, & Mushotzky 1993; Reynolds 1997). In addition, according to Nandra & Pounds (1994), this source exhibits a “hard tail” (or hard X-ray excess) above 10 keV. This soft and/or hard excess is model dependent and is especially sensitive to a continuum slope. Hence, an accurate measurement of continuum slope in a wide energy range is essential for understanding these excess phenomena. At present, it is not yet clear whether the soft excess in MCG–2-58-22 is transient or stable or whether the excess itself exists.

The second problem is that the measured continuum slope has so far been different from observatory to observatory. For instance, it has been reported that the time-averaged continuum of MCG–2-58-22 can be described by a simple power-law with a spectral index of  $\Gamma \approx 2.1$  in a ROSAT energy band and with  $\Gamma \approx 1.75$  in an ASCA energy range (e.g., Turner, George, & Mushotzky 1993; Weaver et al. 1995; Piro, Matt, & Ricci 1997). The energy-dependent spectral slope is unclear and it is yet to be seen whether it is real or due to a limited pass-band. There is an iron line centered at  $\sim 6.2$  keV (e.g., Nandra &

Pounds 1994 and Weaver et al. 1995). Moreover, according to Turner et al. (1991) and Turner, George, & Mushotzky (1993), there is a soft X-ray line at  $\sim 0.8$  keV. Finally, X-ray flux of MCG–2-58-22 is known to vary by a factor of 4, from  $\sim 1 \times 10^{44}$  to  $\sim 4 \times 10^{44}$  ergs  $\text{s}^{-1}$  (2–10 keV), but little is known about the nature of the time variations. Ghosh & Soundararajaperumal (1992) examined the spectral variability with EXOSAT data, and they concluded that soft X-ray is subject to change with the flux variation, and consequently magnitude of the soft excess also varies. This result is still remained to be confirmed.

In this paper, we examine these problems in detail. In § 2 we describe the ROSAT and ASCA observations as well as the data reduction procedures. In § 3 we analyze light curves and obtain some new results for their time variability. Fitting of the combined ROSAT and ASCA spectra is performed in § 4. Using the model of the combined spectra, we also investigate a spectral variability in § 4 for data that were obtained from different observations. Finally, we discuss the results of our study in § 5.

## 2. OBSERVATIONS AND DATA REDUCTION

ROSAT observations of MCG–2-58-22 were made four times from 1991 to 1993 as listed in Table 1. These pointed observations were carried out with the Position Sensitive Proportional Counter (PSPC-B) with an on-axis spatial resolution of about 20 arcsec (Pfefferman et al. 1986). PSPC is sensitive in a 0.1–2.0 keV energy range and has a field of view of 2 degrees. Energy resolution of the PSPC is approximated by  $\Delta E/E = 0.43(E/0.93)^{-0.5}$  in a full-width at half-maximum (FWHM), where  $E$  is in keV.

The ROSAT data were retrieved through the High Energy Astrophysics Science Archive Research Center (HEASARC) on-line service, provided by the NASA/Goddard Space Flight Center. Among the available data, both data sets of 1991 November 21 (rp700107)

and 1993 May 21 (rp701250) were partly analyzed and published by, e.g., Turner, George, & Mushotzky (1993) and Piro, Matt, & Ricci (1997), but other data have not been yet. All the available data are included in this study. Data reduction was performed with the FTOOLS v4.2 software package in our study (Turner 1996). Source photons are extracted from a circular region of about 2 arcmin centered on the source, and the background data are obtained from annular source-free regions in the same field of view.

MCG–2-58-22 was also observed by ASCA three times during the period of 1993 to 1997 (Table 1). Particularly, ASCA and ROSAT were pointed at this source simultaneously on 1993 May 25–26 for about 2.3 hrs. Some results of this ASCA data set were already published by several researchers, including Weaver et al. (1995), Reynolds (1997) and Nandra et al. (1997a, 1997b). Nevertheless, we use this data set in order to do an analysis for combined ROSAT and ASCA spectra. However, other sets of ASCA data still remain to be analyzed.

The ASCA satellite has 4 focal plane instruments, two of which are Solid-State Imaging Spectrometers (SIS0 & SIS1) and the other two are Gas Imaging Spectrometers (GIS2 & GIS3). Each of the SISs consists of 4 CCD chips with an FWHM energy resolution of  $\sim 60 - 120$  eV in the 0.4–10 keV energy range at launch time (Burke et al. 1993), while the GISs have an energy resolution of  $\sim 200 - 600$  eV in the 0.8–10 keV range (Ohashi et al. 1996; Makishima et al. 1996). The SISs in 1 CCD mode provide an 11 arcmin  $\times$  11 arcmin square field of view, while the GISs give a circular field of view with a diameter of 50 arcmin, regardless of their observational mode.

We acquired ASCA data from the HEASARC public archives. In order to avoid possible X-ray contamination from the bright Earth and regions of high particle background, we apply standard data-screening procedures: (1) data are rejected for SISs and GISs when the pointing direction of the telescope is less than  $30^\circ$  and  $8^\circ$  from the Earth's limb,

respectively, (2) only the regions where the radiation-belt monitor has a count rate less than 300 count/s are selected for SISs, (3) regions of cutoff rigidity larger than 10 GeV/c are selected for both of the instruments. Hot and flickering pixels are also removed from the SIS data. Then, source photons are extracted from a circular region of about 4 arcmin centered on the source. Background data are extracted from the high-latitude, blank sky data publicly available.

### 3. LIGHT CURVES AND TIME VARIABILITIES

It is well known that time variability in X-ray intensity is a common characteristic of AGNs, which ranges from hours to years. According to the recent studies by Nandra et al. (1997a) and Ptak et al. (1998), there is a clear anti-correlation between X-ray luminosities and magnitude of time variabilities in Seyfert 1 galaxies. MCG–2-58-22 is a bright Seyfert ( $L_X \sim 10^{44}$  ergs s $^{-1}$ ) deficient of rapid time variations, although it is known to be variable by a factor of 4 on time scales of years. We study the variability of MCG–2-58-22 on both short and long time scales.

Figure 1 shows six light curves extracted from the ROSAT/PSPC (left panels; 0.1–2.0 keV) and the ASCA/GIS data (right panels; 0.8–10 keV). In the figure, GIS2 and GIS3 data were averaged and each data point was binned in 300 s intervals. The X-ray background, which is negligible in the plot, was not subtracted. Among the light curves, we clearly see a steady increase of the X-ray flux (0.1–2.0 keV) in the ROSAT light curve of 1993 May 21–26 (MJD 49128–49138; left-middle panel). We performed the  $\chi^2$  test against the hypothesis of a constant X-ray flux, which resulted in a  $\chi^2$  value of  $\chi^2/\nu$  (degree of freedom) = 325.2/110. The hypothesis is clearly rejected; X-ray flux from MCG–2-58-22 is variable within the time scale of a few days. To understand the nature of the variability, we investigated energy-dependent light curves obtained in the 0.1–0.9 keV band and the

0.9–2.0 keV band. We confirmed that a similar pattern of the flux increase was seen in the both energy bands. The calculated  $\chi^2$  values against a constant flux were  $\chi^2/\nu = 213.6/110$  (0.1–0.9 keV) and  $\chi^2/\nu = 230.6/110$  (0.9–2.0 keV), respectively.

Exposure times of the ROSAT observations of 1991 November 21 (MJD 48581) and 1993 December 1 (MJD 49322) were too short for a  $\chi^2$  test. Instead, we closely looked at the light curves. From the visual inspection, we found a significant short-term variation in the light curve of 1991 November 21 (Figure 2). It is clear from the figure that there is a sudden increase and decrease of flux, from 3.9 counts/s to 4.4 counts/s, at the observation time of 19.2 hr. This variation has a time scale of  $\sim 10^3$  s. We also closely examined the light curve of 1993 December 1, but could not find such a rapid variation. We calculated the  $\chi^2$  values (against the constant hypothesis) for the three sets of the ASCA light curve in Figure 1. The calculated  $\chi^2$  values for the ASCA light curves are  $\chi^2/\nu = 103.9/87$  for the 1993 May observation (MJD 49133–49134), and 149.6/98 and 106.6/102, respectively, for the 1997 June and December observations. Only the light curve in 1997 June shows statistically significant time variation. The variation may have a similar time scale as the ROSAT data in 1993 May, although statistics of the ASCA data are not good enough to investigate the energy dependence. We also see a factor of 2 change in the GIS flux (0.8–10 keV) between 1993 and 1997 observations. ASCA light curve of 1993 May was also analyzed by Nandra et al. (1997a), and they obtained the same conclusion as ours.

In addition to the above light curves, we have also made a long-term light curve (2–10 keV). As explained in the subsequent section, the spectral shape of MCG–2-58-22 is weakly dependent on its flux level in a 2–10 keV band. Therefore, we assumed a power-law ( $\Gamma = 1.7$ ) modified by the low-energy absorption ( $N_H = 2.3 \times 10^{20} \text{ cm}^{-2}$ ), which explains both ASCA and ROSAT energy spectra simultaneously (see Table 2 and § 4.3 to convert the ROSAT count rate into a 2–10 keV flux). For the long-term light curve,

we have also included ROSAT all-sky survey data (Voges et al. 1999), as well as those calculated from previous studies (open circles in the figure; Turner et al. 1991; Ghosh & Soundararajaperumal 1992; Nandra & Pounds 1994). The result is shown in Figure 3, which covers about 18 yrs from 1979 to 1997. We see a long-term change of the flux, which decreased gradually from 1979 through 1993 but increased afterward. One interesting point is that there is a flare-like event in 1991 November; the flux is at least three times larger than that expected from the long-term trend between 1979 and 1993. Because we have only a single set of observation, it is difficult to estimate the true magnitude and duration of the flare-like event. However, the time scale may be less than a few years and the flux increased by at least a factor of 3.

## 4. SPECTRAL ANALYSES AND THE RESULTS

### 4.1. Fitting of Combined ROSAT and ASCA Spectra

It has been reported that the time-averaged continuum of MCG–2-58-22 can be described by a simple power-law model, i.e., power-law  $\times$  Galactic absorption, with a spectral index of  $\Gamma \approx 2.1$  in the ROSAT energy band and of  $\Gamma \approx 1.75$  in the ASCA energy band (e.g., Turner, George, & Mushotzky 1993 and Weaver et al. 1995). In addition, there is an iron line feature around 6–7 keV (Nandra & Pounds 1994; Weaver et al. 1995). In order to examine whether this energy-dependent spectral slope is real, we combine ROSAT and ASCA spectra. As mentioned in § 2, the two observatories pointed at MCG–2-58-22 at the same time for about 2.3 hrs. Therefore, we use these data to avoid any temporal spectral change effect. The spectra shown in Figure 4 were extracted separately from the PSPC, SIS and GIS data, and the background was subtracted. In this process, we added the two energy spectra from SIS0 and SIS1, and simultaneously from GIS2 and GIS3, to improve statistics.

We first attempt to fit the combined spectra with the simple power-law model (model 1). In this fit, normalization of each instrument is allowed to vary independently, but other parameters such as spectral index  $\Gamma$  and hydrogen equivalent column density  $N_H$  are linked together. The resulting  $\chi^2$  in Table 2 implies that the combined spectra can be fitted by a single power-law in a wide range of 0.1–10 keV relatively well. Some residual structure is recognized around 6–7 keV, but the spectral ratio between the data and the model continuum does not show any significant soft X-ray excess (upper panel of Figure 5). This means that there may be little difference in spectral slope between the soft (ROSAT) and the hard (ASCA) spectra. However, the measured column density in the line of sight to the source,  $N_H = 2.2_{-0.5}^{+0.4} \times 10^{20} \text{ cm}^{-2}$ , is slightly smaller than the Galactic value  $3.5 \times 10^{20} \text{ cm}^{-2}$  (e.g., Piro, Matt, & Ricci 1997). If  $N_H$  is fixed to the Galactic value (model 2), it results in a soft X-ray excess below about 0.5 keV as shown in the lower panel of Figure 5. Increase of  $\chi^2$  was also significant. This result suggests that if one sticks to the Galactic absorption column, one has to include an additional spectral component to explain the soft excess. As an alternative test, we applied different absorption model such as an ionized or warm absorber model (“absori” in the XANADU/XSPEC package), but found it does not affect the above results significantly. For instance, when the parameters of “absori” were allowed to be free, spectral index and column density parameters converged to the values of model 1, which uses photo-electric absorption cross-sections of Morrison & McCammon (1983).

Although the simple power-law model gave an acceptable fit from a statistical point of view, we note a residual structure around 6–7 keV, which is broad and weak but significant (Figure 5). This is suggestive of an emission line. Because the presence of an emission line might affect the estimation of the power-law slope and the hydrogen equivalent column density, we tried to fit a third model to the combined data. Considering both this structure and previous reports on the detection of iron line from MCG–2-58-22, we add a Gaussian to the power-law model: (power-law + Gaussian)  $\times$  low-energy absorption (model 3). We

tried only the simplest line model because of relatively poor statistics of the data. Solid lines in Figure 4 represent the best-fit model, and the best-fit parameter values and their uncertainties at the 90% confidence limit are listed in Table 2. In this fit, we did not correct the red-shift effect and assumed a broad iron line and fixed the Gaussian width to  $\sigma = 0.9$  keV (§ 4.2). By including the Gaussian, we could obtain a substantially improved fit as shown in Table 2. Based on the line parameters, we calculate the line flux to be  $1.1_{-0.5}^{+0.4} \times 10^{-12}$  ergs cm $^{-2}$  s $^{-1}$ . The best-fit power-law slope is similar to that of model 2, and the hydrogen equivalent column density is found to be  $N_H = 2.3_{-0.3}^{+0.5} \times 10^{20}$  cm $^{-2}$ , which is slightly smaller than the Galactic value. Thus the inclusion of an iron-K line does not resolve the discrepancy between the best-fitting column density and the Galactic column. We will return to this problem in § 4.3.

## 4.2. Iron Line Study

According to the recent study by Nandra et al. (1997b), most of the Seyfert 1 galaxies observed with ASCA show broad iron K $\alpha$  lines with a mean width of  $\sigma = 0.43 \pm 0.12$  keV. In addition, some UV emission lines, Ly $\alpha$  and C $_{\rm IV}$  (1549 Å), are measured to be broad for MCG–2–58–22 ( $\sim 5000$  km s $^{-1}$  at FWHM in the rest frame; Türler & Courvoisier 1998). In practice, an accurate determination of the line parameters is difficult with the above ASCA spectrum, because of the weakness of the line structure and the relatively poor data statistics in higher energy range. Here we examine iron line properties further with ASCA/SIS data that obtained in 1997 June and 1997 December for longer exposure. Because we found no significant difference between the energy spectra at these two epochs, we added the two spectra to improve the statistics.

In the course of data analysis, we realized that the radiation damage effect is significant in the lower energy range ( $< 1.5$  keV) of SIS data (Hwang et al. 1999; Yaqoob 2000). To

demonstrate the effect, we first fit the model 3 (Table 2) to the GIS data with all the parameters fixed except for the normalization and confirmed that the model can fit the data very well. Then, we calculated a PHA ratio of the SIS spectrum to model 3, which is shown in Figure 6. As seen from the figure, SIS data become significantly smaller than the model below 1.5 keV. This is due to the radiation damage to SIS. Because this effect is not included in the current calibration data yet, we just discard the SIS data below 1.5 keV.

To see the iron line structure first, we calculate spectral ratio between the summed SIS data and the model continuum, which is shown in Figure 7. This figure shows a broad structure between 5–8 keV, implying the presence of a broad iron line. If we apply a single Gaussian model to the line, we obtain an acceptable fit with the best-fit line width of  $\sigma = 0.9^{+0.6}_{-0.3}$  keV (Table 3). On the other hand, if we apply a disk line model to investigate the origin of the broadness, we get a similar goodness of fit (Table 3). We have fixed some of the parameters in the disk line model, to which the  $\chi^2$  value is not very sensitive, in the fitting. The fitting results indicate that, although the line profile is very different between the broad Gaussian and the disk line models, current data do not have good enough statistics to distinguish the line profiles. In fact, we could not constrain the disk line parameters very well. Because there already exists detailed study of the iron feature in MCG–2–58–22 (Weaver et al. 1995; Nandra et al. 1997b), we do not further elaborate on the study of the iron feature in the present paper.

### 4.3. Soft-Band Variability

As we can see in Figure 7, there is little difference in the continuum spectrum between the 1993 and the 1997 data. This means that although there is a factor of 2 change in X-ray flux, this flux variation does not accompany any spectral change in 2–10 keV. However, this does not necessarily mean that the spectral shape is also stable in lower energy band.

Because ASCA/SIS cannot be used to look at the long-term spectral change below 2 keV due to the accumulating radiation damage, we concentrate on the ROSAT data in this subsection.

As we did in § 4.2, we calculate spectral ratios for the ROSAT data taking model 3 (with the best-fit parameters to the combined ROSAT and ASCA data) as a reference (Figure 8). The ratio may be constant for 1993 December data, but a clear structure is seen in 1991 November data. A similar structure, but less pronounced, is also recognized in 1993 May data. It is clear from Figure 8 that either (or both) of the column density or the power-law index is time variable. To identify the variable component, we fit a power-law model with the low-energy absorption to the ROSAT PSPC spectra, and calculated confidence contour plots. The results are summarized in Table 4 and in Figure 9. For clarity, we did not plot the confidence contour for the data in 1993 December, which gave only a very loose constraint to the parameters.

We can see from the confidence contours that the energy spectra clearly have a steeper slope than that determined by the ASCA data. The photon index determined by ASCA in 1.5–10 keV is  $1.73 \pm 0.04$ , whereas the PSPC required the photon index to be larger than 1.8 (1993 May 24–25) and 1.9 (1993 May 21–23, 1991 November 21). Most probable photon index in PSPC band is 2.1. As explained in § 4.1, we succeeded in fitting the combined ASCA and ROSAT spectra by a simple absorbed power-law model. The result is not necessarily in contradiction to the result in this subsection, because the statistics of the combined ASCA/ROSAT spectra were not very good. Furthermore, even if the power-law slope in the ROSAT band is allowed to be time variable, acceptable range of the absorption column is, although marginal, smaller than the Galactic value at least for the data in 1991 November. We interpret this result as implying that the energy spectrum of MCG–2–58–22 in ROSAT band is not a simple absorbed power-law, but has more complex structures. The

structures may be time variable, and are probably correlated with the flux level. When the X-ray flux is large, the soft band spectrum tends to become steeper, which results from either a larger photon index or a lower column density.

## 5. DISCUSSION

We have analyzed the ROSAT and ASCA archive data of MCG–2-58-22. From the long-term light curve covering from 1979 through 1993, we found a flare event in 1991 November overlaid on the gradual change of the X-ray flux. The X-ray flux increased at least a factor of 3 during the flare. Although the time scale of the flare is not known, it is less than about a year. We also detected a very rapid time variation of a relative amplitude of about 10% with a time scale of  $10^3$  s. Energy spectra of MCG–2-58-22 were found to be rather complex. Iron-K line is significantly broad, and soft band spectra (0.1–2 keV) contain some structures, which cannot be reproduced by a simple absorbed power-law. But the energy resolution and statistics of the current data may not be enough to study the iron line and the low energy structures in detail. We discuss the origin of the time variabilities first and then the structures in the energy spectra.

### 5.1. Origins of Time Variabilities in MCG–2-58-22

The long term modulations with occasional flares in the light curves of some AGNs are mostly seen in the optical range. The long term X-ray light curve of MCG–2-58-22 we obtained appears interestingly similar to some of the long term optical light curves. The large amplitude flares and gradual long term modulations could imply that these systems are undergoing at least two distinctly different physical processes differing in time scales and spatial locations. Webb (1990) reported the results of 61 years of optical observations

of 3C120 and claimed that a gradual and possibly sinusoidal variability component of period 12.43 yrs as well as high amplitude flares on much shorter time scales. This behavior is very similar to that of MCG–2-58-22 we obtained. It is also interesting to point out that Dibai & Lyutyi (1984) claimed that AGN such as NGC 3516 and others essentially have two variability time scales, 10–30 day flares and 10–30 yr sinusoidal variation, which appear to be similar to those in other long-term variability studies.

If the variabilities arise from the viscous and dynamical processes in accretion disks in galactic nuclei, the characteristic time scales can be as long as years which correspond to the outermost regions of accretion disks. Observations in various bands suggest that a wide range of variability time scales exist, which in turn indicates a wide range of distance scales associated with various emission components. It has been often discussed that the long term ( $\sim$  yrs – a few  $\times$  10 yrs) variabilities are caused by some types of tidal interaction while the short term variabilities have been attributed to the accretion emission regions.

One of the possible origins of the long term variabilities is the dynamic changes in emissions regions in terms of the re-distribution of matter and resulting variable emission and/or self-absorption. There are a number of relevant time scales operating in the accretion disk around a massive black hole in the galactic nucleus (Frank et al. 1992 and references therein). The typical dynamical time scale for a Keplerian disk is

$$t_{dyn} \sim 3 \times 10^{-2} (M/10^7 M_\odot)^{-1/2} (R/10^{15} \text{ cm})^{3/2} \text{ yr}, \quad (5-1)$$

where  $M$  is the mass of the black hole and  $R$  is the distance from the black hole. This time scale would provide a long term variability of a few yr to ten yrs for  $R > 10^{16}$  cm, although the exact mechanisms responsible for such variabilities remain somewhat uncertain. The viscous time scale on which the disk material's density is modulated is much longer than the dynamical time scale, i.e.,

$$t_{vis} \sim R^2/\nu$$

$$\begin{aligned}
 &\sim \alpha^{-1} (H/R)^{-2} t_{dyn} \\
 &\sim 10^3 (\alpha/0.1)^{-1} [(H/R)/0.1]^{-2} t_{dyn} \\
 &\gg t_{dyn},
 \end{aligned}$$

where  $\nu$  is the kinematic viscosity coefficient,  $\alpha \sim 0.1 - 1$  is the dimensionless viscosity parameter, and  $H$  is the disk's vertical pressure scale height. The thermal fluctuations in the disk operate on the thermal time scale

$$t_{th} \sim 10(\alpha/0.1)^{-1} t_{dyn}, \quad (5-2)$$

which falls between the viscous time scale and the dynamical time scale. If the disk experiences a viscous-thermal instability, which is caused by the sudden change of hydrogen ionization in the disk at an effective disk temperature  $T_{eff} \sim 4000$  K. The viscous-thermal instability time scale is roughly estimated as

$$t_{vis-th} \sim 3 \times 10^2 (\alpha/0.1)^{-1} (M/10^7 M_\odot)^{1/3} (\dot{M}/10^{-4} M_\odot/\text{yr})^{1/3}, \quad (5-3)$$

which is a relevant time scale for mass accretion rate modulation on long time scales. These time scales imply that there in principle exists a large range of time scales on which mass accretion rate ( $\dot{M}$ ) and emission can be modulated.

The origin of flare-like modulations such as the one we detected in MCG–2-58-22 have not been convincingly accounted for. One of the possible mechanisms is the disruption of stars in the tidal field of the massive black hole (e.g., Cannizzo et al. 1990). In a closely related process, a star could plunge into the accretion disk and drag-heat the accretion disk creating a sudden episode of heating and emission (e.g., Hall et al. 1996 and references therein), although the frequency, duration, and intensity of such encounters depend on many detailed dynamical as well as plasma physical details which are beyond the scope of this paper. As in some Galactic binary systems, the accretion disk could have a hot scattering corona which Compton-upscatters the lower energy photons emitted by the

accretion disks. Any such coronal model for X-ray emission requires an electron acceleration mechanism such as magnetic flares and dissipation driven by magnetic field buoyancy and reconnection. Such a process is inherently flare-like and it occurs on relatively short time scales (e.g., Di Matteo, Blackman, & Fabian 1997). The detailed theoretical discussions and their observational signatures will be presented elsewhere.

We detected very rapid time variation as short as  $10^3$  s from MCG–2-58-22. Nandra et al. (1997a) studied such ultra-rapid variability for a sample of 18 Seyfert 1 galaxies using the ASCA data. They detected significant power at frequencies greater than  $10^{-3}$  Hz in at least five sources. However, unequal sampling and poor statistics of the data make it difficult to detect such ultra-rapid variabilities in most cases. In fact, although their analysis sample included MCG–2-58-22, they could not detect ultra-rapid variability. It is known that there is a good correlation between the X-ray variability amplitude and the source luminosity (Nandra et al. 1997a; Turner et al. 1999). Because MCG–2-58-22 is a bright Seyfert ( $L_{2-10\text{keV}} = 1 - 4 \times 10^{44}$  ergs  $\text{s}^{-1}$ ), it shows relatively low amplitude of time variation. However, we found an ultra-rapid variability from MCG–2-58-22. This may be interpreted as implying that high frequency variabilities ( $> 10^{-3}$  Hz) is common to Seyfert galaxies, but the present observations do not have a sensitivity high enough to detect them. Most rapid time variations in X-ray flux may be expected from the inner most region of the accretion disk, which corresponds to 3 times the Schwarzschild radius ( $6GM/c^2$ ). The dynamical time scale ( $t_{dyn}^{in}$ ) at this radius is:

$$t_{dyn}^{in} \sim 8 \times 10^2 (M/10^7 M_\odot) \text{ s.} \quad (5-4)$$

This is comparable to the observed time scale. Although we do not know the mass of the central black hole in MCG–2-58-22, the ultra-rapid variabilities ( $\sim 10^3$  s) may be produced at the vicinity of the event horizon of the black hole.

## 5.2. Structures in the Energy Spectra

We found that the energy spectra of MCG–2-58-22 in 0.1–10 keV cannot be reproduced all the times by a simple power-law modified by the low energy absorption. Energy spectra above  $\sim$ 2 keV gives a photon index of 1.73, whereas lower energy spectra (0.1–2 keV) prefer a photon index of 2.1. Furthermore, if we fit a power-law ( $\Gamma = 2.1$ ) to 0.1–2 keV spectra, the best-fitting absorption column becomes lower than the Galactic value. If we force the Galactic absorption, some of the energy spectra cannot be fit by the absorbed power-law model. We also found that the low energy spectra of MCG–2-58-22 is not stable, but show significant time variations. Therefore, depending on the statistics of the data, an simple power-law with a low energy absorption may give statistically acceptable fit to 0.1–10 keV data. However, if the data have good statistics, such a simple model may be rejected from the statistical point of view. We consider a possibility that the time variations of the low energy structures may be the main source of complexities in the spectral shape of MCG–2-58-22.

There are several possible origins for the low energy structures. Low energy spectra of selected Seyfert 1 galaxies (including MCG–2-58-22) are studied in reference to the Ginga analysis (Piro et al. 1997). The models they tried include “warm absorber”, “reflection from mildly ionized material”, and a blackbody components, but none of these models gave satisfactory fits to all the data; combination of two components might be needed. Zdziarski et al. (1999) found a very strong correlation between the intrinsic spectral slopes and the amount of Compton reflection from a cold medium in Seyferts and in the hard state of X-ray binaries. Objects with softer intrinsic spectra tend to have much stronger reflection structure. Because MCG–2-58-22 has a relatively hard intrinsic spectra ( $\Gamma = 1.67 \pm 0.08$ ; Nandra & Pounds 1994), only a small reflection structure may be expected in its energy spectrum. In fact, Nandra & Pounds (1994) found little reflection structure in

the Ginga spectrum of MCG–2-58-22. Although these considerations may prefer such an interpretation that the structures in the energy spectra of MCG–2-58-22 are more closely related to the warm absorber, we consider that the available data sets are not enough to draw clear conclusion.

We detected a broad iron line from MCG–2-58-22. Both a simple Gaussian and a disk line model gave a similarly good fit to the data, and we could not investigate the line profile in detail. However, as shown in Figure 7, the line is clearly dominated by a broad component, and the contribution of a narrow line, if present, is small. Iron-K line profiles were investigated as a function of X-ray luminosity in AGNs (Nandra et al. 1997c). The line strength clearly decreases with increasing luminosity. Furthermore, the line profiles also changed; narrow Gaussian component largely disappeared above  $L_X \sim 10^{45}$  ergs s $^{-1}$  (2–10 keV). MCG–2-58-22 has an X-ray luminosity of  $1 - 4 \times 10^{44}$  ergs s $^{-1}$ . Thus the line profile may lack the narrow component, which is consistent to the line profile we obtained (Figure 7).

## 6. SUMMARY AND CONCLUSION

Our analyses of MCG–2-58-22 X-ray data have yielded the following results:

1. The 1979–1997 X-ray light curve clearly exhibits a long term variability. A flare-like event is detected in 1991 overlaid over the gradual flux variations.
2. The observed variability time scales span a wide range from  $10^3$  s to years. The most rapid variability we detected is as short as  $10^3$  s, which could be related to the dynamical time scale at the inner most region of the accretion disk.
3. The combined ROSAT and ASCA energy spectra may not be reproduced by an absorbed power-law model, so long as the Galactic absorption of  $3.5 \times 10^{20}$  cm $^{-2}$

is adopted. Energy spectra in ROSAT band (0.1–2.0 keV) requires either a steeper continuum or a lower absorption.

4. The observed spectra in the energy range of 0.1–2.0 keV are clearly time variable.
5. There exists a broad iron line centered at  $\sim 6.3$  keV.

Origin of the short term flare event on top of the gradual X-ray flux modulation remains unresolved. It is interesting that similar flare-like events have been reported in the optical light curves of some AGNs which also show gradual modulations on time scales of years and tens of years. There exist some interesting physical time scales which naturally arise in accretion disks around supermassive black holes. However, it has not been accounted for how the flares of these time scales are produced.

Energy spectra of MCG–2-58-22 are quite complex. Iron-K line is noticeably broad, and soft band spectra (0.1–2 keV) contain some significant structures, which cannot be accounted for by a simple absorbed power-law. Although it is possible that the low energy structures are more closely related to the warm absorber, the presently available data sets are not good enough to draw a definite conclusion.

## REFERENCES

Burke, B. E., Mountain, R. W., Daniels, P. J., Cooper, M. J., & Dolat, V. S. 1993, Proc. SPIE, 2006, 272

Cannizzo, J. H., Lee, H. M., & Goodman, J. 1990, ApJ, 351, 38

Dibai, E. A. & Lyutyi, V. M. 1984, Soviet Astron., 28, 7

Di Matteo, T., Blackman, E. G., Fabian, A. C. 1997, MNRAS, 291, 23

Frank, J., King, A. R., & Raine, D. 1992, Accretion Power in Astrophysics (Cambridge: Cambridge Press)

Ghosh, K. K., & Soundararajaperumal, S. 1992, ApJ, 398, 501

Hall, S. M., Clarke, C. J., & Pringle, J. E. 1996, MNRAS, 278, 303

Hwang, U., Mushotzky, R. F., Burns, J. O., Fukazawa, Y., & White, R. A. 1999, ApJ, 516, 604

Huchra, J., Latham, D. W., Costa, L. N., Pellegrini, P. S., & Willmer, C. N. A. 1993, AJ, 105, 1637

Kotilainen, J. K., & Martin, J. W. 1994, MNRAS, 266, 953

Makishima, K. et al. 1996, PASJ, 48, 171

Mushotzky, R. F. 1984, Adv. Space Res., 3, 10

Morrison, R., & McCammon, D. 1983, ApJ, 270, 119

Nandra, K., & Pounds, K. A. 1994, MNRAS, 268, 405

Nandra, K., George, I. M., Mushotzky, R. F., Turner, T. J., & Yaqoob, T. 1997a, ApJ, 476, 70

---

————— 1997b, ApJ, 477, 602.

---

————— 1997c, ApJL, 488, 91.

Ohashi, T., et al. 1996, 48, 157

Pfeffermann, E., et al. 1986, Proc. SPIE, 733, 519

Piro, L., Matt, G., & Ricci, R. 1997, A&AS, 126, 525

Ptak, A., Yaqoob, T., Mushotzky, R. F., Serlemitsos, P., & Griffiths, R. 1998, ApJ, 501, L37.

Reynolds, C. S. 1997, MNRAS, 286, 513

Türler, M., & Courvoisier, T. J. -L. 1998, A&A, 329, 863

Turner, T. J. 1996, ROSAT Data Analysis Using Xselect and Ftools (OGIP Memo OGIP/94-010)

Turner, T. J., George, I. M., & Mushotzky, R. F. 1993, ApJ, 412, 72

Turner, T. J., George, I. M., Nandra, K., & Turcan, D. 1999, ApJ, 524, 667

Turner, T. J., & Pounds, K. A. 1989, MNRAS, 240, 833

Turner, T. J., Weaver, K. A., Mushotzky, R. F., Holt, S. S., & Madejski, G. M. 1991, ApJ, 381, 85

Voges, W. et al. 1999, A&A, 349, 389

Weaver, K. A., Nousek, J., Yaqoob, T., Hayashida, K. A., & Murakami, S. 1995, ApJ, 451, 147

Webb, J. R. 1990, AJ, 99, 49

Whittle, M. 1992, ApJS, 79, 49

Yaqoob, T. 2000, <http://lheawww.gsfc.nasa.gov/~yaqoob/ccd/nhparam.html>

Zdziarski, A. A., Lubiński, P., & Smith, D. A. 1999, MNRAS, 303, L11

Table 1: THE ROSAT AND ASCA OBSERVATIONS OF MCG–2–58–22

DATA <sup>1</sup>	OBSERVATION (DATE)	INSTRUMENT	EXPOSURE <sup>2</sup>	COUNT RATE <sup>3</sup>
			(ks)	(c/s)
rp700107	1991 November 21	PSPC-B	3.5	4.0
rp701250	1993 May 21–25	PSPC-B	18.7	0.9
rp700998	1993 May 24–26	PSPC-B	10.6	1.0
rp701364	1993 December 1	PSPC-B	2.2	0.7
ad70004000	1993 May 25–26	GIS, SIS	23.3	0.4
ad75049000	1997 June 1–2	GIS, SIS	26.3	0.9
ad75049010	1997 December 15–17	GIS, SIS	29.8	0.9

<sup>1</sup> Sequential number of archival data.

<sup>2</sup> Net exposure times after the data screening. In the case of ASCA observations, the exposures are from the GIS.

<sup>3</sup> Mean source count rates before the subtraction of the background are from PSPC and GIS.

Table 2: BEST-FIT RESULTS FOR THE COMBINED ROSAT AND ASCA SPECTRA

PARAMETERS	BEST-FIT VALUES		
	model 1 <sup>a</sup>	model 2 <sup>b</sup>	model 3 <sup>c</sup>
$\Gamma$	$1.69^{+0.03}_{-0.03}$	$1.73^{+0.02}_{-0.02}$	$1.73^{+0.04}_{-0.04}$
$N_H$ ( $10^{20}$ cm $^{-2}$ )	$2.2^{+0.4}_{-0.5}$	3.51	$2.3^{+0.5}_{-0.3}$
Normalization for PSPC ( $10^{-3}$ )	$4.0^{+0.2}_{-0.2}$	$4.2^{+0.2}_{-0.2}$	$4.0^{+0.2}_{-0.2}$
Norm. for SIS ( $10^{-3}$ )	$3.73^{+0.07}_{-0.07}$	$3.86^{+0.07}_{-0.07}$	$3.77^{+0.08}_{-0.08}$
Norm. for GIS ( $10^{-3}$ )	$4.6^{+0.2}_{-0.1}$	$4.8^{+0.1}_{-0.1}$	$4.7^{+0.2}_{-0.1}$
$E_K$ <sup>d</sup> (keV)	...	...	$6.0^{+0.6}_{-0.5}$
$\sigma$ <sup>e</sup>	...	...	0.9
$I_{Fe}^f$ ( $10^{-4}$ photons cm $^{-2}$ s $^{-1}$ )	...	...	$1.1^{+0.4}_{-0.3}$
EW <sup>g</sup> (keV)	...	...	$0.6^{+0.2}_{-0.3}$
$\chi^2/\nu$	82.4/114	106.1/115	69.1/112
Flux <sup>h</sup> (0.1–2.0 keV)	1.1	...	1.1
Flux <sup>h</sup> (2.0–10 keV)	1.7	1.7	1.7

NOTE.— Errors are 90% confidence level for a single parameter.

Best-fit parameters are not corrected for the red shift ( $z = 0.04732$ )

<sup>a</sup> model 1 = power-law  $\times$  Galactic absorption.

<sup>b</sup> model 2 = power-law  $\times$  Galactic absorption, where  $N_H$  is fixed as the Galactic value.

<sup>c</sup> model 3 = (power-law + Gaussian)  $\times$  Galactic absorption.

<sup>d</sup> Iron line center energy.

<sup>e</sup> Intrinsic line width is fixed.

<sup>f</sup> Calculated iron line flux.

<sup>g</sup> Equivalent width of the iron line.

<sup>h</sup> Calculated mean continuum flux in units of  $10^{-11}$  ergs cm $^{-2}$  s $^{-1}$ .

Table 3: BEST-FITTING PARAMETERS FOR THE ASCA SPECTRUM

PARAMETERS	BEST-FIT VALUES	
	GAUSSIAN LINE	DISK LINE
$\Gamma$	$1.73^{+0.04}_{-0.03}$	$1.73^{+0.03}_{-0.03}$
$N_H^a$ ( $10^{20}$ cm $^{-2}$ )	2.3	2.3
Normalization ( $10^{-3}$ )	$9.0^{+0.3}_{-0.2}$	$9.0^{+0.2}_{-0.2}$
$E_K$ (keV)	$6.3^{+0.7}_{-0.4}$	$6.1^{+0.5}_{-0.4}$
$\sigma$	$0.9^{+0.6}_{-0.3}$	...
$R_{in}$ (GM/c $^2$ )	...	$< 40$
$R_{out}$ (GM/c $^2$ ) $^b$	...	1000
Inclination (deg) $^b$	...	90
$I_{Fe}$ ( $10^{-4}$ photons cm $^{-2}$ s $^{-1}$ )	$1.8^{+1.2}_{-0.6}$	$1.8^{+0.8}_{-0.7}$
EW (keV)	$0.5^{+0.3}_{-0.2}$	$0.5^{+0.2}_{-0.2}$
$\chi^2/\nu$	20.4/34	21.1/34
Flux $^c$ (2.0–10 keV)	3.5	3.5

NOTE.— Errors are 90% confidence level for a single parameter. The red-shift effect is not corrected.

 $^a$  Fixed as the value of the combined spectra (Table 2). $^b$  Fixed in the spectral fitting. $^c$  Calculated continuum flux in units of  $10^{-11}$  ergs cm $^{-2}$  s $^{-1}$ .

Table 4: BEST-FITTING RESULTS FOR THE ROSAT SPECTRA

PARAMETERS	1991 November 21	1993 May 21-23	1993 May 24-25	1993 December 1
$\Gamma$	$2.10^{+0.09}_{-0.09}$	$2.1^{+0.1}_{-0.1}$	$2.1^{+0.2}_{-0.2}$	$2.1^{+0.4}_{-0.4}$
$N_H$ ( $10^{20}$ cm $^{-2}$ )	$3.0^{+0.3}_{-0.3}$	$3.5^{+0.5}_{-0.4}$	$3.6^{+0.7}_{-0.6}$	$3.2^{+1.8}_{-1.4}$
Normalization ( $10^{-3}$ )	$14.1^{+0.4}_{-0.3}$	$3.4^{+0.1}_{-0.1}$	$3.8^{+0.2}_{-0.2}$	$2.5^{+0.3}_{-0.3}$
$\chi^2/\nu$	14.2/21	6.7/21	14.9/21	5.9/21
Flux <sup>a</sup> (0.1–2.0 keV)	39.3	9.2	10.1	7.0

NOTE.— Errors are 90% confidence level for a single parameter.

<sup>a</sup> Calculated continuum flux in units of  $10^{-12}$  ergs cm $^{-2}$  s $^{-1}$ .

## FIGURE CAPTIONS

Fig. 1.— X-ray light curves of MCG–2-58-22 obtained from the ROSAT/PSPC (left panels; 0.1–2.0 keV) and the ASCA/GIS observations (right panels; 0.8–10 keV). Data from GIS2 and GIS3 are averaged in the plots. Light curves are calculated in 300 s bin for all the data sets, and no background was subtracted.

Fig. 2.— Part of the ROSAT light curve of MCG–2-58-22 during the 1991 November 21 observation, when the source showed a very rapid time variation. Data were binned in 300 s intervals.

Fig. 3.— Long-term X-ray light curve of MCG–2-58-22 obtained in a 2–10 keV band. Filled and open circles in the figure represent the flux data calculated in the current study and those adopted from the literature, respectively. The dashed lines are included for the convenience of the interpretation.

Fig. 4.— Average energy spectra of MCG–2-58-22 observed in 1993 May 25–26. In this figure, each spectrum was rebinned appropriately to give better statistics per bin. Then the model function, (power-law + Gaussian line)  $\times$  low-energy absorption, was fitted to the PSPC, SIS and GIS spectra simultaneously. The solid lines represent the best-fit model function.

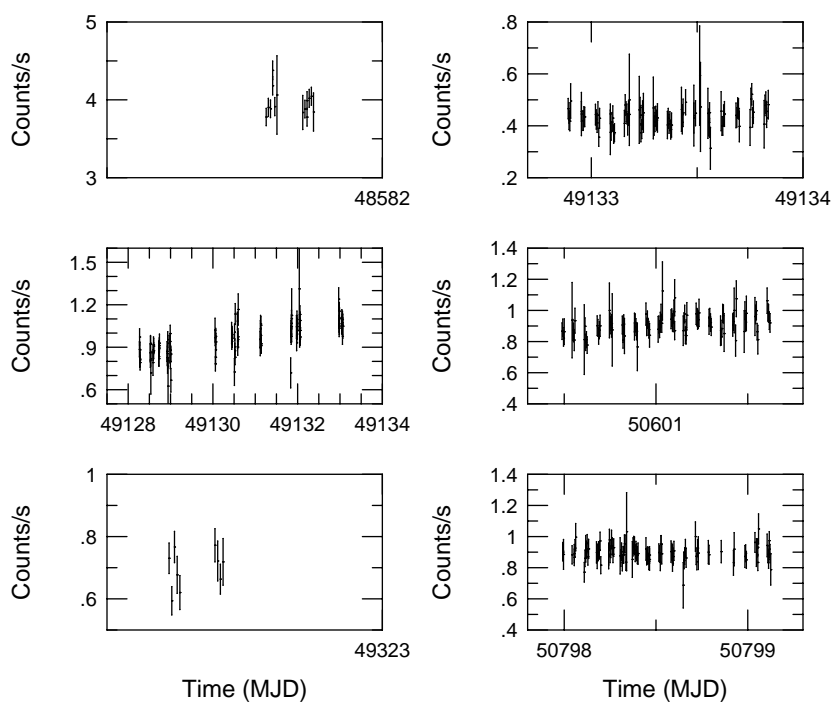
Fig. 5.— Spectral ratio of the combined ROSAT/ASCA spectra to the continuum models. The upper and lower panels take the model 1 and the model 2 (see text) as the reference, respectively. Both panels show a weak and broad residual structure around 6–7 keV, implying the presence of an iron line. In addition, the lower panel clearly shows soft X-ray excess below about 0.5 keV to the model.

Fig. 6.— Residuals of the ASCA spectra of 1997 June to the best-fit model of the combined spectra. This figure displays a considerable discrepancy between the SIS spectrum and the model below 1.5 keV, which increases with decreasing energy. The deviations are ascribed to the reduction of quantum efficiency in SIS by radiation damage.

Fig. 7.— Spectral ratio between the ASCA/SIS spectrum and the best-fit model continuum of the combined spectra (model 3 in Table 2). This figure clearly shows the presence of a broad iron line.

Fig. 8.— Spectral ratio of the ROSAT spectra to the best-fit model of the combined spectra (model 3 in Table 2).

Fig. 9.— Confidence contours (68%, 90%, and 99% levels) for power-law photon index vs. hydrogen equivalent column density for a fit to the ROSAT PSPC spectra. Solid lines and short-dashed and long-dashed lines are for the spectra of 1991 November 21, 1993 May 21–25, and 1993 May 24–26, respectively.



MGC-2-58-22

